CIRCUITS SYSTEMS SIGNAL PROCESSING
VOL. 25, NO. 3, 2006, PP. 295–314

DOI: 10.1007/s00034-004-0819-3

NONLINEAR TRANSIENT AND DISTORTION ANALYSIS VIA FREQUENCY DOMAIN VOLTERRA SERIES*

Junjie Yang[1] *and Sheldon X.-D. Tan*[2]

Abstract. This paper presents a novel approach for transient and distortion analyses for time-invariant and periodically time-varying mildly nonlinear analog circuits. Our method is based on a frequency domain Volterra series representation of nonlinear circuits. It computes the nonlinear responses using a nonlinear current method that recursively solves a series of linear Volterra circuits to obtain linear and higher-order responses of a nonlinear circuit. Unlike existing approaches, where Volterra circuits are solved mainly in the time domain, the new method solves the linear Volterra circuits directly in the frequency domain via an efficient graph-based technique, which can derive transfer functions for any large linear network efficiently. As a result, both frequency domain characteristics, like harmonic and intermodulation distortion, and time domain waveforms can be computed efficiently. The new algorithm takes advantage of identical Volterra circuits for second- and higher-order responses, which results in significant savings in driving the transfer functions. Experimental results for two circuits—a low-noise amplifier and a switching mixer—are obtained and compared with SPICE3 to validate the effectiveness of this method.
Key words: Nonlinear transient simulation, distortion analysis, Volterra series.

1. Introduction

Transient analysis of nonlinear analog circuits is the most computationally intensive analysis. Linear multistep (LMS) formulas based on backward difference formulas [10] are widely used methods for transient simulation of nonlinear circuits

* Received August 19, 2004; revised August 10, 2005; Some preliminary results of this paper appear in the *Proc. IEEE International Symposium on Circuits and Systems* (ISCAS), Vancouver, Canada, May 2004. This work is partly supported by the University of California Senate Research Funds.

[1] Formerly with Department of Electrical Engineering, University of California, Riverside, California 92521, USA; now with Nulife Technology Corp., 2975 Scott Blvd., Suite 109, Santa Clara, California 95054, USA. E-mail: jyang@ee.ucr.edu

[2] Department of Electrical Engineering, University of California, Riverside, California 92521, USA. E-mail: email:stan@ee.ucr.edu

due to their robustness. The *predictor-corrector algorithms*, with explicit LMS formulas for the predictor and an implicit LMS formula for the corrector, can be used to further speed up the transient simulation. These methods are general enough for both mildly and hard nonlinear circuits. But because Newton-Raphson iterations are carried out at every time step of integration, these algorithms are very time consuming. If only a steady-state response is required, some special analysis methods for nonlinear circuits have been developed such as harmonic balance methods in the frequency domain and shooting methods in the time domain [2], [1].

For wireless/communication applications, some circuits which operate at radio frequencies (RF) typically exhibit mildly or weakly nonlinear properties, where devices typically have a fixed dc operating point or periodically changed operating points and the inputs are ac signals. When the amplitude of these input signals is small (such that the operation points do not change too much), the nonlinearities in these circuits can be approximated adequately using a truncated Taylor series expansion of the nonlinear devices at their dc operating points [11].

Such mild nonlinearities can be exploited to speed up the transient simulation for such nonlinear circuits [4]. Examples are the linear centric method for nonlinear distortion analysis [3] and the sampled-data simulation method using Volterra functional series [13]. Volterra functional series can represent a weakly nonlinear function in terms of a number of linear functions called Volterra kernels. From circuit theory's perspective, it leads to a set of linear circuits, called Volterra circuits, whose responses can adequately approximate the response of the original nonlinear circuit. In [13], [14], a sampled-data simulation method is used where the simulation errors are dependent on sampling intervals and sampling window sizes. As a result, the runtime is dependent on the accuracy requirements. It is also difficult to obtain frequency domain information such as harmonic distortions as the algorithm operates in the time domain.

In this paper, we propose a new approach for transient and distortion analysis of time-invariant and periodically time-varying mildly nonlinear analog circuits. Our method is also based on the Volterra functional series. But instead of solving the Volterra circuits in the time domain, as in traditional methods like SPICE3 or the sampled-data method [13], [14], we solve the Volterra circuits directly in the frequency domain by using a graph-based symbolic analysis method [6], [7]. Once frequency domain responses are obtained, transient responses can be obtained by efficient numerical inverse Fourier transformation of all frequency components. The new method is more efficient than time domain nonlinear analysis as the analysis is done in the frequency domain which is independent of time intervals and time steps, and no convergence issues of nonlinear iterations (like Newton-Raphson) are involved. Another significant benefit is that we can easily obtain frequency domain characteristics like harmonic distortions and intermodulations as they can be easily computed from the frequency responses of various orders of Volterra circuits. Experimental results for some real nonlinear circuits are studied

and compared with those of SPICE3 to validate the new method. Both transient and second and third harmonic distortion (HD2, HD3) and intermodulation results are computed for each nonlinear circuit to show the effectiveness of the new method.

2. Volterra circuits and determinant decision diagram graphs review

2.1. Volterra circuits

A time-invariant nonlinear circuit can be expressed by the following differential equations:

$$Gv(t) + C\frac{dv(t)}{dt} = Dw(t) + i_{non}(v(t)). \tag{1}$$

Here G and C represent, respectively, the conductance and capacitance matrices whose elements are made of the linear devices and first-order terms of the Taylor series expansion of the nonlinear devices. D is the position vector for input $w(t)$. $i_{non}(v(t))$ represents the second- and higher-order currents generated by the nonlinear devices. By substituting Volterra functional series of $v(t)$ and $i(t)$ into the equation, we will obtain a set of linear differential equations [4], [13]:

$$\begin{aligned}
Gv_1(t) + C\frac{dv_1(t)}{dt} &= Dw(t),\\
Gv_2(t) + C\frac{dv_2(t)}{dt} &= i_2(v_1(t)),\\
Gv_3(t) + C\frac{dv_3(t)}{dt} &= i_3(v_1(t), v_2(t)),\\
&\cdots\\
Gv_m(t) + C\frac{dv_m(t)}{dt} &= i_m(v_1(t), v_2(t), \ldots, v_{m-1}(t)),
\end{aligned} \tag{2}$$

where $v_m(t)$ is the mth-order term of the Volterra series expansion of $v(t)$ and $i_m(t)$ is the input of the mth-order Volterra circuit and can be obtained from lower-order responses: $v_{m-1}(t), v_{m-2}(t), \ldots, v_1(t)$.

For a given nonlinear circuit, we assume that currents are nonlinear functions of voltages for nonlinear devices. The i-v characteristic of the nonlinear device can be expanded at the dc operating point as a Taylor series,

$$\begin{aligned}
I(V) &= I_0 + i\\
&= f(V_0) + \sum_{n=1}^{\infty} \frac{f^n(V_0)}{n!} v^n = I_0 + \sum_{n=1}^{\infty} a_n v^n,
\end{aligned} \tag{3}$$

where I_0 and V_0 represent the dc current and voltage values over the nonlinear device, and i and v represent the corresponding small signal voltage and current

values, respectively. Hence, i can be expressed as a polynomial function in v with coefficients a_i, $i = 1, \ldots, n$. For Volterra functional series, if the input is changed from $v(t)$ to $\lambda v(t)$, we have [4]

$$v(t) = \sum_{m=1}^{\infty} v_m(t)\lambda^m, \qquad i(t) = \sum_{m=1}^{\infty} i_m(t)\lambda^m. \tag{4}$$

Substituting equation (3) into (4), we have

$$\sum_{m=1}^{\infty} i_m(t)\lambda^m = \sum_{n=1}^{\infty} a_n \Big(\sum_{m=1}^{\infty} v_m(t)\lambda^m\Big)^n. \tag{5}$$

Equating terms of the same order in λ, we obtain

$$i_m(t) = a_1 v_m(t) + J_m(t), \tag{6}$$

where $J_m(t)$ is the contribution from the responses of low order (less than m) Volterra circuits. But for $m = 1$, $J_m(t) = 0$. Equation (6) essentially reflects the fact that each Volterra circuit is a linear circuit (a_1 is used for all the Volterra circuits for the nonlinear device), and higher-order responses can be computed in an order-increasing way starting from the first order. The response of the whole circuit will be the sum of the responses from all the Volterra circuits.

2.2. *The DDD graph-based method for deriving transfer functions*

In this subsection, we briefly review a graph-based method, called determinant decision diagrams (DDDs), to derive the exact transfer functions of a linear circuit [5]. DDDs [5] are compact and canonical graph-based representations of determinants. DDD graphs are similar to binary decision diagrams (BDDs) except that a sign is associated with each node to represent the sign of product terms from the expansion of a determinant. Also like BDDs, DDDs can be used to represent huge numbers of symbolic terms from a determinant. Most importantly, one can derive the s-expanded polynomial of a determinant symbolically via s-expanded DDDs [6]. The recent hierarchical approach using DDD graphs can essentially derive transfer functions for almost arbitrary large networks [7], which makes the solving of linear networks in the frequency domain much easier and more efficient.

The concept is best illustrated using the simple RC filter circuit shown in Figure 1. Its system equations can be written as

$$\begin{bmatrix} \frac{1}{R_1} + s\mathbf{C_1} + \frac{1}{R_2} & -\frac{1}{R_2} & 0 \\ -\frac{1}{R_2} & \frac{1}{R_2} + sC_2 + \frac{1}{R_3} & -\frac{1}{R_3} \\ 0 & -\frac{1}{R_3} & \frac{1}{R_3} + s\mathbf{C_3} \end{bmatrix} \begin{bmatrix} v_1 \\ v_2 \\ v_3 \end{bmatrix} = \begin{bmatrix} I \\ 0 \\ 0 \end{bmatrix}.$$

Author: Bold roman C_1, C_3 like in previous equation?

Let $\underline{C_1}$ and C_3 be two symbolic parameters in the circuit. Matrix entries $\frac{1}{R_1} +$

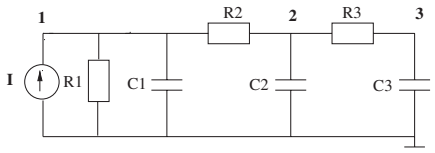

Figure 1. A simple RC circuit.

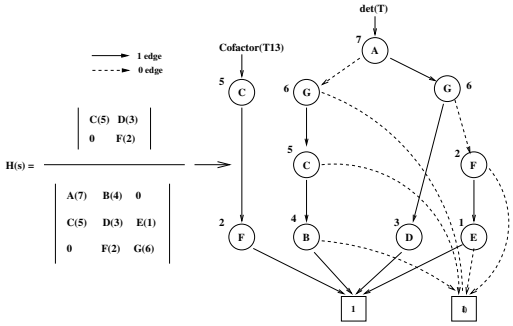

Figure 2. A complex preordered DDD for the transfer function.

$sC_1 + \frac{1}{R_2}$ and $\frac{1}{R_3} + sC_3$ will be assigned indices larger than the indices of all other entries to make them appear on the top of the corresponding DDD graph. Let T be the 3×3 system matrix; we are interested in the following transfer function:

$$H(s) = \frac{V_3(s)}{I(s)} = \frac{(-1)^{1+3} \det(T_{13})}{\det(T)}, \tag{7}$$

where T_{13} is the matrix obtained by removing row 1 and column 3 from T. The resulting determinant of the system matrix, its cofactor T_{13}, and their DDD representations are shown in Figure 2, where each nonzero element is designated by a symbol and is assigned a unique index in parentheses. The index of each symbol is also marked along each DDD node in the resulting DDD graph. It can be seen that symbolic nodes A and G appear above all the other numerical DDD nodes.

Once complex DDDs are obtained, s-expanded DDDs are can be computed very efficiently [6]. Consider again the circuit in Figure 1 and its system determinant. Let us introduce a unique symbol for each circuit parameter in its admittance form. Specifically, we introduce $a = \frac{1}{R_1}, b = f = \frac{1}{R_2}, d = e = -\frac{1}{R_2}$, $g = k = \frac{1}{R_3}, i = j = -\frac{1}{R_3}, C_1 = c, h = C_2, l = C_3$. Then the circuit matrix can be rewritten as

$$\begin{bmatrix} a+b+\mathbf{c}s & d & 0 \\ e & f+g+hs & i \\ 0 & j & k+\mathbf{l}s \end{bmatrix}.$$

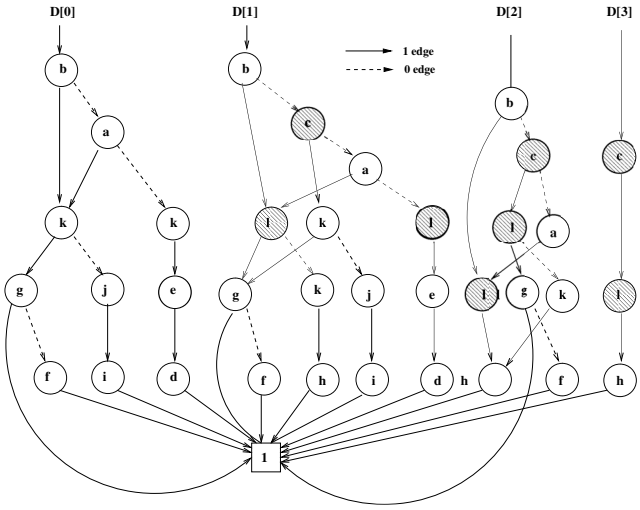

Figure 3. Semi-symbolic s-expanded DDDs for $\det(T)$.

The corresponding s-expanded DDDs are shown in Figure 3.

3. Frequency domain Volterra circuits

In this section, we will first illustrate the representation of frequency domain Volterra circuits for general time-invariant weakly nonlinear systems. We then discuss the representation of periodically time-varying nonlinear systems.

For the time-invariant nonlinear system expressed in equation (2), we can take a Fourier transform on both sides of the differential equations:

$$\begin{aligned} GV_1(jw) + jwCV_1(jw) &= DW(jw), \\ GV_2(jw) + jwCV_2(jw) &= I_2(jw), \\ GV_3(jw) + jwCV_3(jw) &= I_3(jw), \\ &\cdots \\ GV_m(jw) + jwCV_m(jw) &= I_m(jw), \end{aligned} \tag{8}$$

where $W(jw)$ is the Fourier transform of input signal $w(t)$, and $V_m(jw)$ and $I_m(jw)$ are those of $v_m(t)$ and $i_m(t)$, respectively. From equation (6), because $J_m(t)$ can be expressed as a sum of product terms of $v_{m-1}(t), v_{m-2}(t), \ldots, v_1(t)$, we can perform convolution in the frequency domain to obtain $I_m(jw)$.

We illustrate this by the following simple example. Consider a nonlinear resistor for which the i-v relationship can be expressed as

$$i(t) = b_1 v(t) + b_2 v^2(t) + b_3 v^3(t). \tag{9}$$

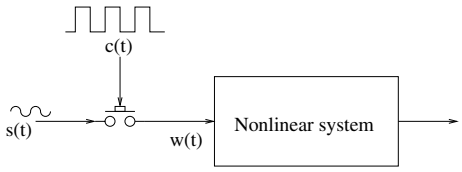

Figure 4. Periodically time-varying nonlinear system model.

From equation (4), the time domain Volterra series $i_m(t)$ are

$$\begin{aligned} i_1(t) &= b_1 v_1(t), \\ i_2(t) &= b_1 v_2(t) + b_2 v_1^2(t), \\ i_3(t) &= b_1 v_3(t) + 2b_2 v_1(t) v_2(t) + b_3 v_1^3(t). \end{aligned} \tag{10}$$

Take the Fourier transform on both sides; we obtain

$$\begin{aligned} I_1(jw) &= b_1 V_1(jw), \\ I_2(jw) &= b_1 V_2(jw) + \frac{1}{2\pi} b_2 V_1(jw) * V_1(jw), \\ I_3(jw) &= b_1 V_3(jw) + \frac{1}{\pi} b_2 V_1(jw) * V_2(jw) \\ &\quad + \frac{1}{4\pi^2} b_3 V_1(jw) * V_1(jw) * V_1(jw), \end{aligned} \tag{11}$$

where $*$ represents the convolution in the frequency domain. In this way, the multiplication in the time domain is converted into the convolution in the frequency domain. We observe that we typically need only a couple of tones of input signals to decide the circuit performance (for example, a one-tone input for harmonic distortion and a two-tone input for intermodulation distortion). The convolution in the frequency domain can be implemented as the shifting product of two signals at all corresponding discrete frequency points,

$$V(kw_0) = V_1 * V_2 = \sum_{m=-N}^{m=N} V_1(mw_0) V_2(kw_0 - mw_0), \tag{12}$$

where N is the number of harmonics we want to consider, which is reasonable because the higher harmonic component can be ignored in most cases. This simplifies the work for nonlinear system analysis by avoiding the time-consuming Fourier transform and inverse Fourier transform between the time domain and frequency domain. It also facilitates the calculation of harmonic and intermodulation distortion because they are frequency domain characteristics.

Now we extend our approach to solve periodically switching nonlinear circuits. As shown in Figure 4, the system can be split into two parts: one for the switching operation and another for the nonlinear operation. The input has two ports: $s(t)$

and $c(t)$. $s(t)$ is a small input signal and $c(t)$ is the controlling signal, usually a square wave. The output $w(t)$ from the switching is

$$w(t) = s(t)c(t). \tag{13}$$

In the frequency domain, it becomes

$$W(jw) = \frac{1}{2\pi} S(jw) * C(jw). \tag{14}$$

When the square wave is the controlling signal, it becomes

$$W(jw) = \sum_{k=-\infty}^{\infty} a_k S(jw + kw_0), \tag{15}$$

where w_0 is the frequency of the square wave, $a_0 = \frac{1}{2}$ when $k = 0$, and $a_k = \frac{\sin(k\pi)}{k\pi}$ when $k \neq 0$. $W(jw)$ is then fed into the nonlinear part for further calculation. We note that many typical analog circuits, such as switching mixer and switching capacitor circuits, can be analyzed very efficiently using this method.

4. New approach to transient and distortion analysis of nonlinear circuits

4.1. Nonlinear analysis flow

From previous analysis on Volterra functional series, we know that all Volterra circuits are linear circuits similar to the original circuit. All second- and higher-order Volterra circuits are the same except that the input current sources are different. As a result, the new method consists of the following steps to obtain the transient response and harmonic and intermodulation distortion of a nonlinear circuit. (1) Based on the nonlinear analytical expressions of the i-v curve for each nonlinear device in the nonlinear circuit, derive the corresponding relationship between i_m and v_m for each of them and generate the corresponding Volterra circuits. (2) Compute the transfer functions for each Volterra circuit using the DDD-based method. Note that only two linear circuits are required; i.e., a circuit for the first-order response and a circuit for the higher-order responses. (3) Add all the frequency/transient responses of different-order Volterra circuits to obtain the frequency/transient responses of the original nonlinear circuit. The transient responses are obtained by using an efficient numerical inverse Fourier transformation [10]. Specific harmonic and intermodulation distortion can be obtained by tone-tracking for a specified frequency at the output of each Volterra circuit of different orders. In the following subsection, we show how to perform harmonic and intermodulation analysis.

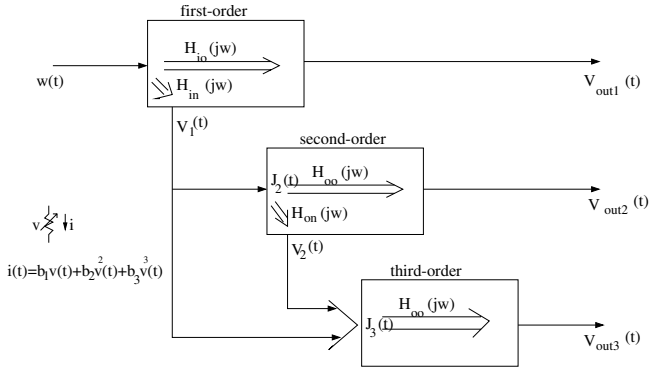

Figure 5. A nonlinear circuit and its first-, second-, and third-order Volterra circuits with linear transfer functions.

4.2. Harmonic and distortion analysis

As usual, we use a one-tone input signal for the harmonic distortion calculation, and a two-tone input signal for the intermodulation analysis. We use the following nonlinear circuit with three-order Volterra circuits to demonstrate how the tone-tracking method is used in our frequency domain analysis framework.

For the nonlinear circuit shown in Figure 5, we include a nonlinear resistor which has the i-v relationship described by equation (9). We calculate the output response from the first-order Volterra circuit. The first-order output is

$$V_{out1}(jw) = W(jw)H_{io}(jw), \tag{16}$$

where $W(jw)$ is the Fourier transform of input signal $w(t)$, and H_{io} is the transfer function from the input to the output for the first-order Volterra circuit. We can obtain the voltage at the nonlinear port as

$$V_1(jw) = W(jw)H_{in}(jw), \tag{17}$$

where $H_{in}(jw)$ is the transfer function from input to nonlinear port for the first-order Volterra circuit. Following equation (11) to obtain $J_2(jw)$, we then calculate the response at the output and nonlinear port for the second-order Volterra circuit,

$$V_{out2}(jw) = J_2(jw)H_{oo}(jw), \tag{18}$$

$$V_2(jw) = J_2(jw)H_{on}(jw), \tag{19}$$

where $H_{oo}(jw)$ is the transfer function from the current source to the voltage at the output and $H_{on}(jw)$ is the transfer function from the current source at the output to the nonlinear port. Both of them are for the second- and higher-order Volterra circuits. Similarly, we can obtain the output for the third-order and higher-order Volterra circuits. Then, by taking into account all the frequency

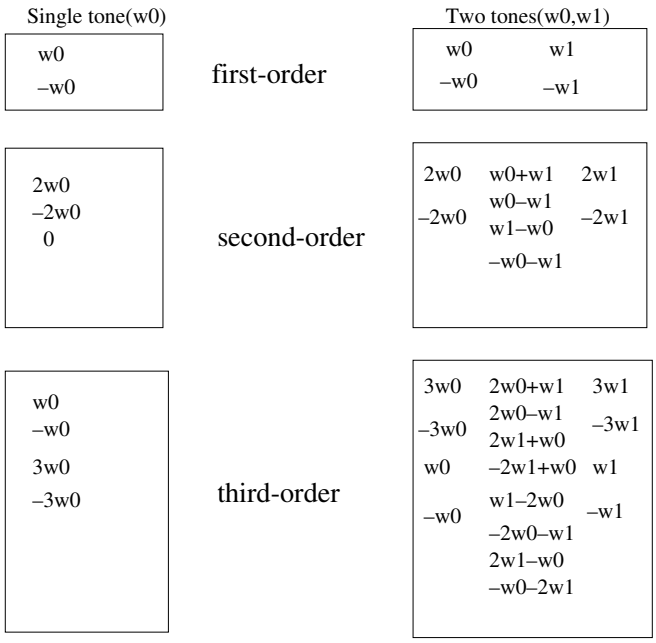

Figure 6. The harmonic and intermodulation frequencies at different-order Volterra circuits with single-tone and two-tone tests.

components for each Volterra circuit, we can easily obtain the transient response for the whole circuit.

Note that only four transfer functions, $H_{io}(jw)$ and $H_{in}(jw)$ for the first-order Volterra circuit and $H_{on}(jw)$ and $H_{oo}(jw)$ for other higher-order Volterra circuits, need to be calculated. The DDD graph-based approach is a very efficient tool for obtaining these transfer functions for very large linear circuits [5], [7]. Because the transfer functions are reused in second- and higher-order Volterra circuits, we achieve significant saving on the calculation of circuit response repeatedly for any higher-order Volterra circuits.

As shown in Figure 6, the signal $w(t)$ containing one frequency component w_0 is the input signal to a general nonlinear system. According to the input-output frequency-invariant property of linear systems and the frequency-shifting property of convolution, we can derive all the frequency components in different-order Volterra circuits. To obtain the second harmonic distortion (HD2), we need to compute the frequency $2w_0$ component contained in the output of the second-order Volterra circuit. From the equation of frequency domain Volterra circuits, the second-order current source is

$$J_2(j2w_0) = b_2 \frac{1}{2\pi} V_1(jw_0) V_1(jw_0). \tag{20}$$

Then the output $V_{out2}(j2w_0)$ of the second-order Volterra circuit can be obtained by the multiplication of $J_2(j2w_0)$ and $H_{oo}(j2w_0)$. The HD2 distortion can be calculated as

$$HD2 = 20\log\left(\frac{|A_{2w_0}|}{|A_{w_0}|}\right), \tag{21}$$

where A_{w_0} is the amplitude of the output signal at frequency w_0 and A_{2w_0} is the second harmonic amplitude at frequency $2w_0$ at the output port.

For the third-order harmonic distortion, we need to consider the frequency component at $3w_0$, contained in the output of the third-order Volterra circuit. There are two signal paths corresponding to the two higher-order items in equation (10): w_0 from $v_1(t)$ and $2w_0$ from $v_2(t)$ for the first item $2b_2v_1(t)v_2(t)$, and three w_0 from $v_1(t)$ for the second item $\underline{b_3v_1(t)^3}$. We have

Author: see equation (10) should be $b_3v_1^3(t)$?

$$\begin{aligned} J_3(j3w_0) = {} & 2b_2\frac{1}{2\pi}V_1(jw_0)V_2(j2w_0) \\ & + b_3\frac{1}{4\pi^2}V_1(jw_0)V_1(jw_0)V_1(jw_0). \end{aligned} \tag{22}$$

Then $V_{out3}(j3w_0)$ can be obtained by the multiplication of $J_3(j3w_0)$ and $H_{oo}(j3w_0)$. The HD3 distortion can be calculated as

$$HD3 = 20\log\left(\frac{|A_{3w_0}|}{|A_{w_0}|}\right), \tag{23}$$

where A_{w_0} is the amplitude of the output signal at frequency w_0 and A_{3w_0} is the third harmonic amplitude at frequency $3w_0$ at the output port.

Now we consider a two-tone input test for the intermodulation calculation. Assume that the input signal only contains two closely located frequency components: w_0 and w_1. The frequency component at $2w_0 - w_1$ at the output is what we are interested in. For the frequency component $2w_0 - w_1$, we have three signal paths corresponding to the two higher-order items: w_0 from $v_1(t)$ and $w_0 - w_1$ from $v_2(t)$, or $-w_1$ from $v_1(t)$ and $2w_0$ from $v_2(t)$ for the first item $2b_2v_1(t)v_2(t)$; and w_0, w_0 and $-w_1$ from $v_1(t)$ for the second item $b_3v_1^3(t)$. It can be written as

$$\begin{aligned} J_3(j(2w_0 - w_1)) = {} & 2b_2\frac{1}{2\pi}V_1(jw_0)V_2(j(w_0 - w_1)) \\ & + 2b_2\frac{1}{2\pi}V_1(-jw_1)V_2(j2w_0) \\ & + b_3\frac{1}{4\pi^2}V_1(jw_0)V_1(jw_0)V_1(-jw_1). \end{aligned} \tag{24}$$

The output $V_{out3}(j(2w_0 - w_1))$ for the third-order Volterra circuit can be obtained by the multiplication of $J_3(j(2w_0 - w_1))$ and $H_{oo}(j(2w_0 - w_1))$. The intermodulation distortion can be calculated as

$$IM3 = 20\log\left(\frac{|A_{(2w_0 - w_1)}|}{|A_{w_0}|}\right), \tag{25}$$

where A_{w_0} is the amplitude of the output signal at frequency w_0 and $A_{2w_0-w_1}$ is the intermodulation amplitude at frequency $2w_0 - w_1$ at the output port.

For periodically time-varying nonlinear circuits, the input signal frequency for the single-tone test is changed from w_0 to $w_0 - kw_s$, where w_s is the frequency of the square wave signal. For the two-tone test, the frequencies at w_0 and w_1 are also shifted by kw_s individually. The procedures are the same for calculating HD2, HD3, and intermodulation when we only consider a limited number of harmonic points (k is limited) and truncate the higher-order harmonic components.

5. Discussion

In this section, we discuss the factors that affect the accuracy and efficiency of our frequency domain method and explore the benefits of this method compared with the time domain method.

5.1. Accuracy

Based on the procedure of the frequency domain method described in the previous section, the accuracy is related to the following factors: (1) the order of the Taylor series characterizing the nonlinear devices, (2) the order of the linear Volterra circuits representing the nonlinear circuits, and (3) the highest order of harmonics considered for the calculation of the frequency domain convolution. These are discussed in more detail as follows.

5.1.1. Order of Taylor series

In our analysis, we use a Taylor expansion to approximate the characteristics of nonlinear devices. For a function $f(x)$ that has continuous derivatioves up to $(n+1)$th order, it can be expanded in the following fashion:

$$f(x) = f(a) + f^{(1)}(a)(x-a) + \frac{f^{(2)}(a)(x-a)^2}{2!} + \frac{f^{(n)}(a)(x-a)^n}{n!} + R_n, \quad (26)$$

where R_n, called the remainder after $n+1$ terms, is given by

$$R_n = \frac{f^{(n+1)}(\eta)(x-a)^{n+1}}{(n+1)!}, \qquad a < \eta < x. \quad (27)$$

In our frequency domain analysis, a is actually our dc operating point. So to keep the remainder R_n in a limited range, the order of the Taylor expansion will rely on the input signal amplitude and the derivative properties of the nonlinear devices themselves.

5.1.2. Order of linear Volterra circuits

In equation (6), for the accurate representation of the Volterra series, m should take values from 0 to infinity. But for an actual mildly nonlinear circuit, we can usually take m as a proper number to meet the corresponding accuracy requirements. As an example, in equation (11), we use third-order Volterra circuits to approximate the original nonlinear circuit. If fourth-order Volterra series are applied for the approximation, the frequency domain representation of the Volterra circuits is

$$\begin{aligned}
I_1(jw) &= b_1 V_1(jw), \\
I_2(jw) &= b_1 V_2(jw) + \frac{1}{2\pi} b_2 V_1(jw) * V_1(jw), \\
I_3(jw) &= b_1 V_3(jw) + \frac{1}{\pi} b_2 V_1(jw) * V_2(jw) \\
&\quad + \frac{1}{4\pi^2} b_3 V_1(jw) * V_1(jw) * V_1(jw), \\
I_4(jw) &= b_1 V_4(jw) + \frac{1}{\pi} b_2 V_1(jw) * V_3(jw) + \frac{1}{2\pi} b_2 V_2(jw) * V_2(jw) \\
&\quad + \frac{3}{4\pi^2} b_3 V_1(jw) * V_1(jw) * V_2(jw). \qquad (28)
\end{aligned}$$

The last item $I_4(jw)$ will be appended to the final solution for higher accuracy, which means the higher-order Volterra circuits will produce more accurate results. But for a mildly nonlinear circuit it can be characterized by low-order Volterra series expansions, usually up to the fifth-order [13].

5.1.3. Harmonic order for convolution calculation

The evaluation of the convolution at the frequency domain can be implemented as the shifting product of two signals at all corresponding discrete frequency points,

$$V(kw_0) = V_1 * V_2 = \sum_{m=-N}^{m=N} V_1(mw_0) V_2(kw_0 - mw_0), \qquad (29)$$

where N is the number of harmonics we want to consider. This is reasonable as the higher harmonic component can be ignored in most cases [9].

Based on the above discussion, we see that all the possible errors can be controllable and negligible in the frequency domain based on the properties of a mildly nonlinear circuit. Compared with the time domain calcaulation, this method avoids the calcaulation of the inverse fast Fourier transform (IFFT) in which process the interpolation error will dominate [13]. From this aspect, we see that this method is more straightforward and that the errors are more controllable than in time domain methods for the evaluation of frequency domain properties of mildly nonlinear circuits, such as distortion and intermodulation.

Author: IFFT means inverse fast Fourier transform

5.2. *Efficiency*

In the analysis flow of the nonlinear circuit, we have stated that the circuit can be approximated as a series of linear Volterra circuits and that second- and higher-order circuits can be taken as the same circuit because they are only different in the current sources. That means we only need to deal with two linear circuits no matter what order Volterra circuits are used for the approximation. The power of the DDD is exploited to expediate this process.

Unlike the exponential growth of product of most symbolic analysis methods, DDD construction takes time almost linear in the number of DDD vertices. For practical analog circuits, the number of DDD vertices is several orders of magnitude less than the number of product terms. It is based on two observations concerning symbolic analysis of large analog circuits: (1) the circuit matrix is sparse and (2) a symbolic expression often shares many subexpressions. Also, the derivation, manipulation, and evaluation of the DDD representations of symbolic determinants have a time complexity proportional to the DDD sizes [5].

Furthermore, compared with the time domain method, the IFFT is avoided, which is usually time consuming and error prone. Also, our method is independent of time intervals and time steps, and no convergence issues of nonlinear iterations (like Newton-Raphson) are involved.

6. Experimental results

We simulate a number of nonlinear analog circuits using the new algorithm. The experimental results are obtained using a PC with 2.4 GHz P-4 CPU and 484 MB memory. Here we report the detailed simulation results for one bipolar low-noise amplifier (LNA) and one switching mixer.

The LNA circuit is shown in Figure 7. First, we obtain the dc conditions with SPICE3 and we get $V_B = V(3) = 0.73$ V, $V_C = V(6) = 4.8$ V, $I_{C1} = 0.19$ mA, and then the ac parameters are computed as follows: $r_b = 1.0\Omega$, $r_\pi = 13.16$ kΩ, $C_u = 133.8$ fF, $C_\pi = 20.66$ fF, $g_m = \frac{I_C}{V_t} = 0.0076$ A/V, $r_o = 510$ kΩ. The ac equivalent circuit is shown in Figure 8 along with the second- and higher-order Volterra circuits.

By using the DDD-based method, we obtain all the required transfer functions,

$$H_{14}(s) = \frac{V_4(s)}{V_1(s)} = \frac{0.0015 - 4.16 \times 10^{-15} s}{0.0002 + 4.60 \times 10^{-15} s + 4.58 \times 10^{-27} s^2},$$

$$H_{13}(s) = \frac{V_3(s)}{V_1(s)} = \frac{0.0002 + 4.16 \times 10^{-15} s}{0.0002 + 4.60 \times 10^{-15} s + 4.58 \times 10^{-27} s^2},$$

where $H_{14}(s)$ and $H_{13}(s)$ are the transfer functions from input node 1 to output node 4 and node 3, respectively. For the second- and higher-order Volterra circuits,

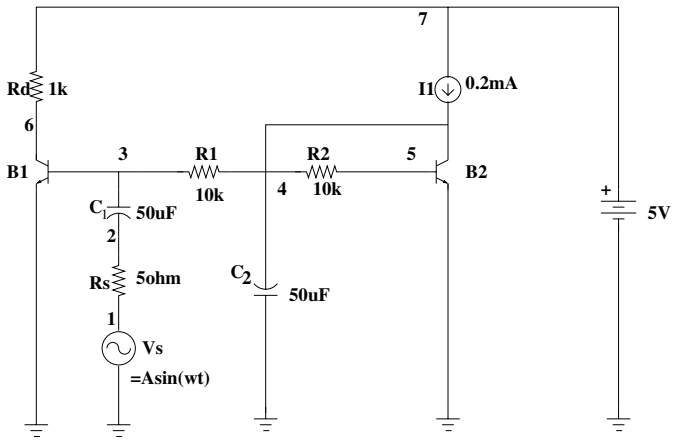

Figure 7. A simple LNA circuit.

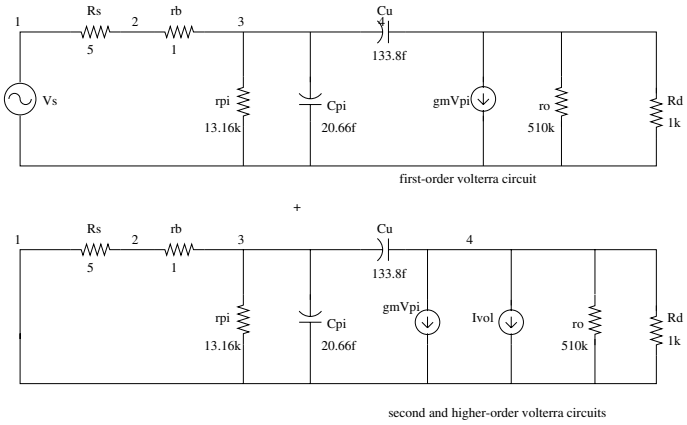

Figure 8. The Volterra circuits for the LNA circuit.

we have

$$H_{44}(s) = \frac{V_4(s)}{I_{vol}(s)} = \frac{0.20 + 2.45 \times 10^{-13}s}{0.0002 + 4.60 \times 10^{-15}s + 4.58 \times 10^{-27}s^2},$$
$$H_{43}(s) = \frac{V_3(s)}{I_{vol}(s)} = \frac{-2.496e - 14s}{0.0002 + 4.60 \times 10^{-15}s + 4.58 \times 10^{-27}s^2},$$

where $H_{44}(s)$ and $H_{43}(s)$ are the transfer functions from the Volterra current source of different orders to output node 4 and node 3, respectively, and I_{vol} is the current source for different-order Volterra circuits.

Following the analysis procedure in Section 4, we obtain the transient response

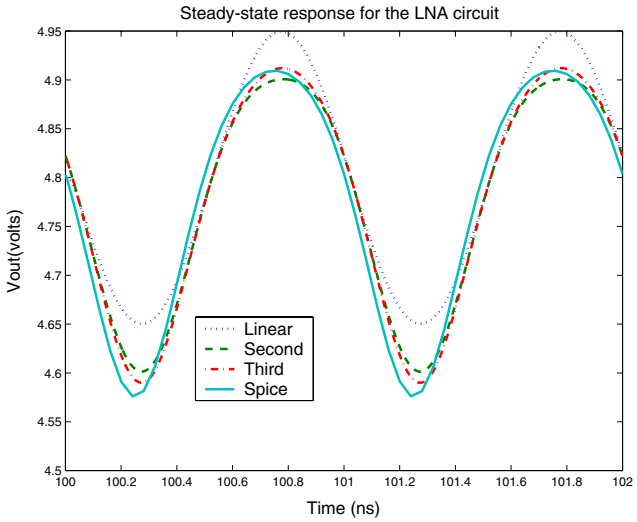

Figure 9. Transient response for the LNA circuit.

shown in Figure 9. The SPICE3 simulated results are also shown and compared with our results. It is clearly seen that the results are in good agreement with each other when the second- and third-order Volterra circuits are considered. HD2 and HD3 are also calculated and are shown in Figure 10. We see that they also coincide with the SPICE3 results. The HD2 and HD3 in SPICE3 are derived from the FFT of a long period of transient simulation for different input signals, which is very time consuming.

The entire computation for driving a 30-ns transient response takes 86 seconds for the new algorithm, while SPICE3 takes 471 seconds to finish the same task. We note that if we increase the time interval and number of time steps, the SPICE3 simulation time will go up accordingly, but our new method will still take the same time, as our approach computes responses in the frequency domain and is independent of time steps and time intervals. Note that if truncation is carried out for very high-order transfer functions, the Hurwitz polynomial [8] can be applied to enforce the stability of the transfer functions if required.

Another example is a switching mixer, as shown in Figure 11. It is composed of a square-wave controlled switch followed by a common-source amplifier. The input V_{rf} is a small signal, and the controlling signal V_{osc} is at 20 MHz. The metal oxide semiconductor (MOS) transistor M1 is simulated as a resistor with an on-resistance of 1 Ω and an off-resistance of 100 MΩ. The dc bias condition for the MOS transistor M2 is: $V(3) = 0$, $V(5) = -1.559$ V, $Vss = -3$ V, $Vdd = 3$ V, $Id = 3.256$ mA. According to the dc analysis, the relationship between the drain

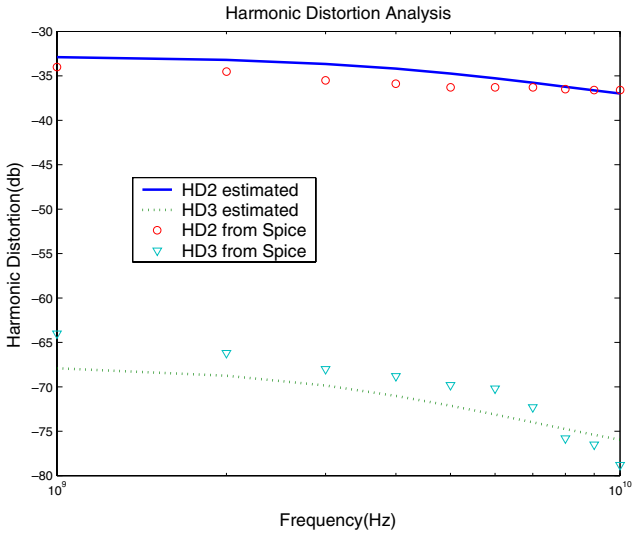

Figure 10. Second and third harmonic distortions (HD2, HD3) for the LNA circuit.

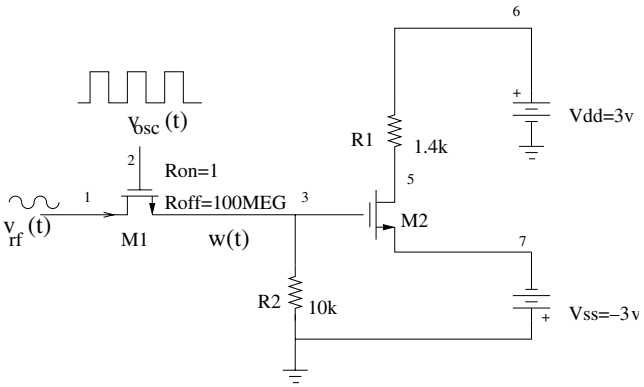

Figure 11. The switching mixer circuit.

current i_d and gate voltage v_g can be represented as

$$i_d = a_1 v_g + a_2 v_g^2 + a_3 v_g^3, \tag{30}$$

where $a_1 = 0.00084542$, $a_2 = -0.0016371$, and $a_3 = 0.0043071$. Also the corresponding ac parameters are calculated as: $g_m = 0.1253$ A/V, $r_o = 1.8$ MΩ, $C_{gd} = 12.1$ fF, $C_{gs} = 328.26$ fF. With our method the simulated transient response is shown in Figure 12, where a sinusoidal signal $V_{rf} = 0.05\sin(2\pi f t)$, $f = 2$ MHz is applied at the RF input port. The

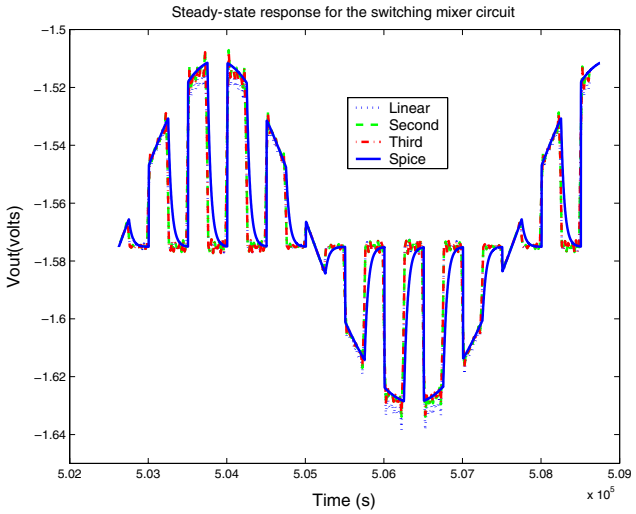

Figure 12. Transient response for the switching mixer circuit.

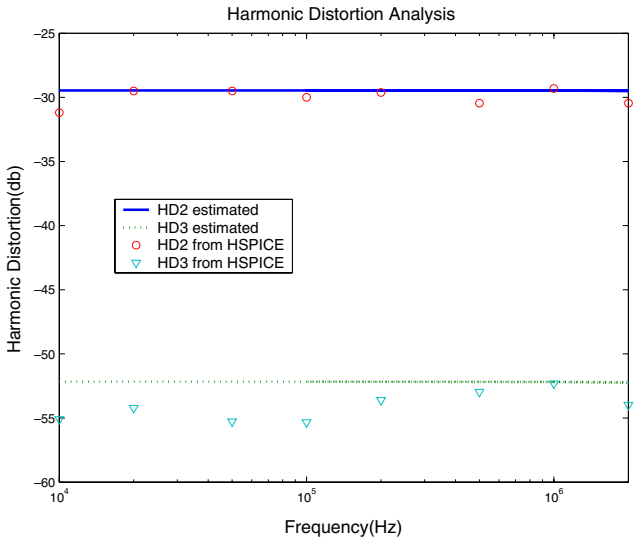

Figure 13. Harmonic distortions (HD2 and HD3) for the switching mixer circuit.

highest harmonic considered is 10th harmonic in this case. The harmonic and intermodulation distortions are shown in Figure 13 and Figure 14, respectively. Both of them are very close to the results calculated from SPICE3.

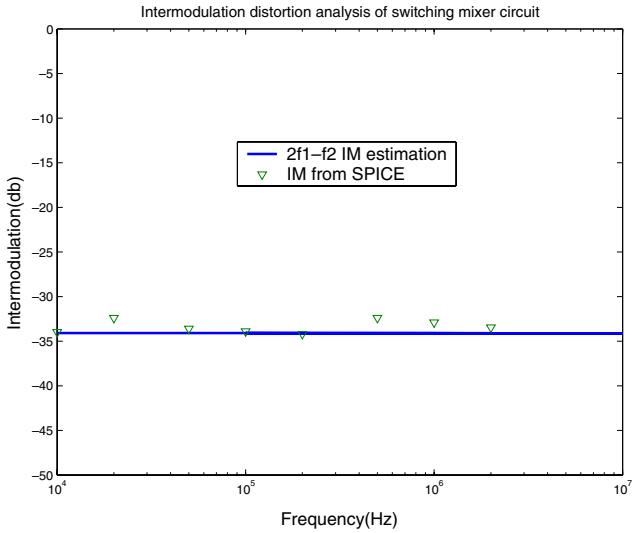

Figure 14. Intermodulation distortion for the switching mixer circuit.

7. Conclusion

In this paper, we have proposed a novel approach for transient and distortion analyses of time-invariance and periodic time-varying mildly nonlinear analog circuits. The new method is based on Volterra functional series. Instead of solving the Volterra circuits numerically in the time domain as traditional methods do, we use a graph-based method to obtain the frequency responses of Volterra circuits of various orders and the tone-tracking method to obtain harmonics and intermodulation distortions in the frequency domain directly. The new method exploits identical Volterra circuit structures for higher-order nonlinear responses and the efficiency of a DDD-based method for deriving transfer functions. Our frequency domain analysis provides many advantages over traditional time domain-based methods in terms of efficiency and easy computation of many frequency domain characteristics. A number of nonlinear analog circuits are simulated using the new method, and the results are compared with that of SPICE3 to demonstrate the effectiveness of the proposed method.

References

[1] J. H. Haywood and Y. L. Chow, Intermodulation distortion analysis using a frequency-domain harmonic balance technique, *IEEE Trans. Microwave Theory Tech.*, vol. 36, pp. 1251–1257, 1988.

[2] K. S. Kundert, J. K. White, and A. Sangiovanni-Vincentelli, *Steady-State Methods for Simulat-*

ing Analog and Microwave Circuits, Kluwer Academic Publishers, Dordrecht, 1990.

[3] P. Li and L. Pileggi, Nonlinear distortion analysis via linear-centric models, *Proc. Asia and South Pacific Design Automation Conference*, pp. 897–903, 2003.

[4] M. Schetzen, *The Volterra and Wiener Theory of Nonlinear Systems*, Wiley, New York, 1981.

[5] C.-J. Shi and X.-D. Tan, Canonical symbolic analysis of large analog circuits with determinant decision diagrams, *IEEE Trans. Computer-Aided Design*, vol. 19, no. 1, pp. 1–18, Jan. 2000.

[6] C.-J. Shi and X.-D. Tan, Compact representation and efficient generation of s-expanded symbolic network functions for computer-aided analog circuit design, *IEEE Trans. Computer-Aided Design*, vol. 20, no. 7, pp. 813–827, July 2001.

[7] S. X.-D. Tan, A general s-domain hierarchical network reduction algorithm, *Proc. IEEE/ACM International Conf. on Computer-Aided Design (ICCAD)*, pp. 650–657, San Jose, CA, Nov. 2003.

[8] S. X.-D. Tan and J. Yang, Hurwitz stable model reduction for non-tree structured RLCK circuits, *Proc. 16th IEEE International System-on-Chip Conference (SOC)*, pp. 239–242, 2003.

[9] P. Vanassche, G. Gielen, and W. Sansen, Symbolic modeling of periodically time-varying systems using harmonic transfer matrices, *IEEE Trans. Computer-Aided Design of Integrated Circuits and Systems*, vol. 21, no. 9, pp. 1011–1024, Sept. 2002.

[10] J. Vlach and K. Singhal, *Computer Methods for Circuit Analysis and Design*, Van Nostrand Reinhold, New York, 1994.

[11] P. Wambacq and W. Sansen, *Distortion Analysis of Analog Integrated Circuits*, Kluwer Academic Publishers, Dordrecht, 1998.

[12] J. Yang and S. X.-D. Tan, An efficient algorithm for transient and distortion analysis of mildly nonlinear analog circuits, *Proc. IEEE International Symposium on Circuits and Systems* (ISCAS), Vancouver, Canada, May 2004.

Author: I don't think ref. [12] was called out in the paper.

[13] F. Yuan and A. Opal, An efficient transient analysis algorithm for mildly nonlinear circuits, *IEEE Trans. Computer-Aided Design of Integrated Circuits and Systems*, vol. 21, no. 6, pp. 662–673, 2002.

[14] F. Yuan and A. Opal, Distortion analysis of periodically switched nonlinear circuits using time-varying Volterra series, *Proc. IEEE International Symposium on Circuits and Systems*, vol. 5, pp. 499–502, 1999.